Bone Reports 18 (2023) 101683

Contents lists available at ScienceDirect

Bone Reports

journal homepage: www.elsevier.com/locate/bonr

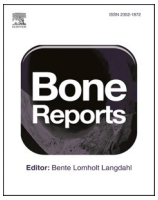

Case Report

Variant of the catalytic cysteine of UFSP2 leads to spondyloepimetaphyseal dysplasia type Di Rocco

Larissa Mattern [a], Matthias Begemann [a], Heide Delbrück [b], Petra Holschbach [c], Silvia Schröder [b], Sabine M. Schacht [d], Ingo Kurth [a], Miriam Elbracht [a,*]

[a] Institute for Human Genetics and Genomic Medicine, Medical Faculty, RWTH Aachen University, Aachen, Germany
[b] Department of Orthopaedic, Trauma and Reconstructive Surgery, Medical Faculty, RWTH Aachen University, Aachen, Germany
[c] Department of Pediatrics, Division of Neuropediatrics and Social Pediatrics, Medical Faculty, RWTH Aachen University, Aachen, Germany
[d] Department of Diagnostic and Interventional Radiology, Medical Faculty, RWTH Aachen University, Aachen, Germany

ARTICLE INFO

Keywords:
UFSP2
Skeletal dysplasia
Spondyloepimetaphyseal dysplasia
UFM1
Beukes hip dysplasia

ABSTRACT

Spondyloepimetaphyseal dysplasia (SEMD) is characterized by vertebral, epiphyseal, and metaphyseal alterations. Patients become predominantly apparent with disproportionate short stature. The genetic background of SEMD is heterogeneous, with different modes of inheritance (autosomal dominant, autosomal recessive, and X-linked disorders). Amongst the genes in which variants are known to cause SEMD, *UFM1-specific protease 2* (*UFSP2*) encodes a cysteine protease involved in the maturation of Ubiquitin-fold modifier 1 (UFM1). Heterozygous pathogenic variants affecting the C-terminal catalytic domain of UFSP2 are related to two entities of skeletal dysplasia, Beukes hip dysplasia (BHD) and SEMD type Di Rocco (SEMDDR). This is the first report of a *de novo* heterozygous variant affecting the catalytic Cys302 residue of *UFSP2* (NM_018359.3:c.905G>C, p.(Cys302Ser)) causing SEMDDR. According to previously described patients with SEMDDR, our patient presented with disproportionate short stature, genu varum, gait instability, and radiologically detected epiphyseal and metaphyseal alterations. Additionally, a bell-shaped thorax, lumbar hyperlordosis, muscular hypotonia, and coxa vara were observed in the patient described in this study. Our findings underline the fundamental importance of an intact catalytic triad of the human UFSP2 for normal skeletal development and extend the phenotypical features of patients with *UFSP2*-related skeletal dysplasia.

1. Introduction

Skeletal dysplasia (SD) represents a broad group of diseases (over 700 distinct entities) in which disease-causing variants in more than 500 genes have been identified to date (Unger et al., 2023). The identification of new pathogenic variants significantly advanced with the increasingly widespread use of massive parallel sequencing. Characterizing genetic variants related to SD is essential to define the diagnosis, prognosis, mode of inheritance, and impact on possible treatment options for the patients. Here, we report a patient with a novel variant in the *UFM1-specific protease 2* (*UFSP2*) gene causing spondyloepimetaphyseal dysplasia type Di Rocco (SEMDDR). There is a phenotypic overlap of the distinct entities in the heterogeneous group of spondyloepimetaphyseal dysplasia (SEMD), consisting of disproportionate short stature with vertebral, as well as metaphyseal and epiphyseal alterations of the long bones. The genetic characterization helps to distinguish between *UFSP2*-related SEMDDR (OMIM# 617974) and differential diagnoses, such as *COL2A1*-related SEMD Strudwick type (SEMD-S, OMIM# 184250).

The *UFSP2* gene encodes a cysteine protease that cleaves the C-terminal extension of Ubiquitin-fold modifier 1 (UFM1), a ubiquitin-like protein (Kang et al., 2007). This proteolytic step leads to the exposure of a highly conserved glycine and is crucial for the subsequent conjugation to target molecules (Komatsu et al., 2004). The structural analysis of UFSP2 using a three-dimensional model of the mouse homolog (Protein Data Bank [PDB]: 3OQC) showed that the protein is composed of two domains, the C-terminal catalytic domain and an N-terminal domain (Fig. 1A) (Kang et al., 2007; Ha et al., 2011).

A homozygous pathogenic variant in the N-terminal domain of UFSP2 (c.344T>A; p.(Val115Glu)) is related to autosomal recessive neurodevelopmental delay and epilepsy (Ni et al., 2021). By contrast, heterozygous missense variants affecting the C-terminal catalytic

* Corresponding author at: Uniklinik RWTH Aachen, Pauwelsstraße 30, 52074 Aachen, Germany.
E-mail address: mielbracht@ukaachen.de (M. Elbracht).

https://doi.org/10.1016/j.bonr.2023.101683
Received 13 February 2023; Received in revised form 2 May 2023; Accepted 3 May 2023
Available online 4 May 2023

domain were found in SD. Watson et al. described a South African family of European descent with UFSP2-related Beukes hip dysplasia (c.868T>C; p.(Tyr290His)) (BHD, OMIM# 142669), a severe premature degenerative osteoarthritis of the hip joints (Cilliers and Beighton, 1990; Watson et al., 2015). The affection of the catalytic triad of UFSP2 results in SEMDDR, which has been reported in three affected individuals of three generations in an Italian family (c.1277A>C; p.(Asp426Ala)) (Di Rocco et al., 2018), and a Chinese boy (c.1283A>G; p.(His428Arg)) (Fig. 1C) (Zhang et al., 2020).

Here, we describe an additional patient with SEMDDR caused by a novel likely pathogenic variant affecting the catalytic cysteine of UFSP2 (c.905G>C; p.(Cys302Ser)). Based on the investigations for mice, it is proposed that the catalytic activities of UFSP2 depend on the catalytic triad composed of Cys294 (corresponding to human Cys302) as well as Asp418 and His428 (corresponding to human Asp426 and His428) in the C-terminus. The importance of the catalytic triad in humans was ascertained by the fact that pathogenic variants affecting the catalytic residues resulted in a loss of activities of UFSP2 (Kang et al., 2007).

2. Clinical report

2.1. Patient data

Our patient is the second son of non-consanguineous parents and was born in the 39th week of gestation after an uneventful pregnancy. One week before delivery, polyhydramnios was recognized. The following birth measurements were collected: weight 3585 g (65th percentile, Z = 0.38), height 49 cm (14th percentile, Z = −1.06), and head circumference 37.5 cm (99th percentile, Z = 2.39). He presented at birth with shortened proximal extremities, a bell-shaped thorax, and a shortened

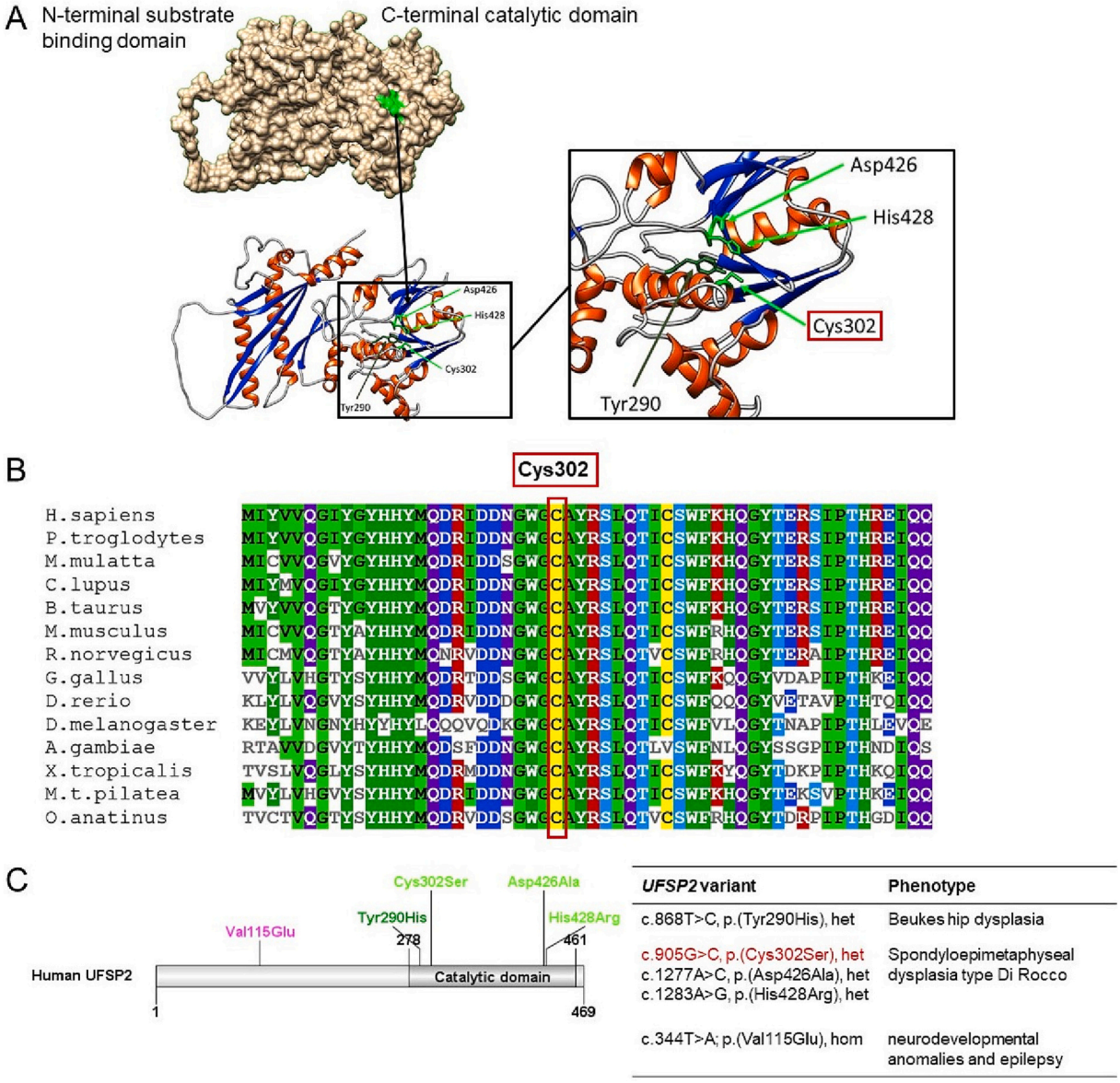

UFSP2 variant	Phenotype
c.868T>C, p.(Tyr290His), het	Beukes hip dysplasia
c.905G>C, p.(Cys302Ser), het c.1277A>C, p.(Asp426Ala), het c.1283A>G, p.(His428Arg), het	Spondyloepimetaphyseal dysplasia type Di Rocco
c.344T>A; p.(Val115Glu), hom	neurodevelopmental anomalies and epilepsy

Fig. 1. Structure of human UFSP2. (A) The human UFSP2 consists of an N-terminal substrate binding domain and a C-terminal catalytic domain. The active site (green) is formed by the catalytic triad consisting of Cys302, Asp426, and His428. The oxyanion hole of the active site consists of the backbone amide of Tyr290 and the catalytic cysteine. (B) The catalytic residue Cys302 is strictly conserved across species. (C) Heterozygous pathogenic variants affecting the catalytic triad Cys302, Asp426, and His428 are related to autosomal dominant spondyloepimetaphyseal dysplasia type Di Rocco. This is the first report of a patient with a variant affecting the catalytic Cys302 residue (highlighted in red). The variant Tyr290His is associated with Beukes hip dysplasia. A homozygous pathogenic variant affecting the N-terminal domain of UFSP2 (p.Val115Glu) is associated with an autosomal recessive form of pediatric neurodevelopmental anomalies and epilepsy without skeletal dysplasia. (het = heterozygous, hom = homozygous.)

sternum (Fig. 2A). Muscular hypotonia and poor spontaneous motor skills were observed. Due to inadequate respiratory adaption, our patient had to be transferred to the pediatric intensive care unit, where he received continuous positive airway pressure (CPAP) respiratory support for three days. The conventional radiological examination did not show any anomalies in thoracic bones (Fig. 3C), and cranial dysmorphism was not described. Abdominal sonography did not reveal organ malformations. The motor development of our patient was delayed, while speech and mental development were not affected. He started crawling at 13 months and learned to run with help at 17 months; however, his gait was very unstable. Free walking was possible at 26 months. The patient was presented to our Social Pediatric Center, where mild muscular hypotonia, lumbar hyperlordosis, and limitation of elbow extension (5°) were diagnosed. Genu varum was treated with thigh-length night positioning splints and thigh-length walking orthoses with knee joint. He showed a slight improvement in motor development with age, while mild muscular hypotonia remained. The family came to our Institute for Human Genetics and Genomic Medicine when the patient was ten months young (Fig. 2B–E).

When the last documented examination took place at 23 months of age, his height was 74 cm (<1st percentile, Z = −3.89), which corresponds to significant growth retardation. The weight was also considerably diminished (8 kg, <1st percentile, Z = −3.34), while the head circumference was in the normal range (49 cm, 69th percentile, Z = 0.49). Conventional radiological examinations of the pelvis with age of 26 months could not delimit epiphyseal nuclei and showed regular horizontal position of the acetabulum without criteria of hip dysplasia. Bilateral dysplasia of the metaphysis of the proximal femur was observed. The lateralization of the bony proximal femur suggests a pronounced coxa vara in this context which was confirmed in the subsequent MRI where the whole femoral head and neck are cartilaginously created. With the current imaging, it is not yet possible to assess whether a femoral neck pseudarthrosis is present or will develop (Fig. 3A, B). The patient's parents and brother do not show any features of SD. The mother's height is 170 cm (85th percentile, Z = 1.031), and the father is 174 cm tall (35th percentile, Z = −0.399). Skeletal anomalies or a significantly reduced body height were also not observed in further relatives. The family originates from western Germany and Poland, respectively.

2.2. Genetic analysis

Genetic analyses were conducted following the local laws concerning genetic diagnostics. Peripheral blood samples of the patient were collected with the consent of the parents. For whole exome sequencing, the xGen Exome Research Panel v2.0 was used to enrich the patient's DNA sample according to the manufacturer's protocol (IDT, Coralville, IA, USA). Sequencing of the exome library was performed on a NextSeq500 Sequencer with 2 × 75 cycles on a high-output flow cell. FastQfiles were generated with bcl2fastq2 (Illumina, San Diego, CA, USA). The automated SeqMule pipeline (v1.2.5) was used for alignment and variant calling (Guo et al., 2015). Variants were detected by the variant caller GATKLite UnifiedGenotyper. KGGSeq (v1.2) was applied for variant annotation and bioinformatics prioritization (Li et al., 2012). Synonymous variants and variants with a minor allele frequency (MAF) greater than 0.75 % in public databases (*i.e.*, gnomAD) were excluded. Pathogenicity of variants was assessed according to ACMG (Richards et al., 2015). Segregation analyses were conducted by Sanger sequencing using an AB3500 platform (Applied Biosystems, USA).

2.3. Protein structure analysis

The three-dimensional human UFSP2 structure (Fig. 1A) was obtained *via* AlphaFold2 (Jumper et al., 2021) and further processed using UCSF Chimera (Pettersen et al., 2004). The colored multiple sequence alignment was designed with MView (Brown et al., 1998), and the linear protein structure was created using DOG 2.0 (Ren et al., 2009).

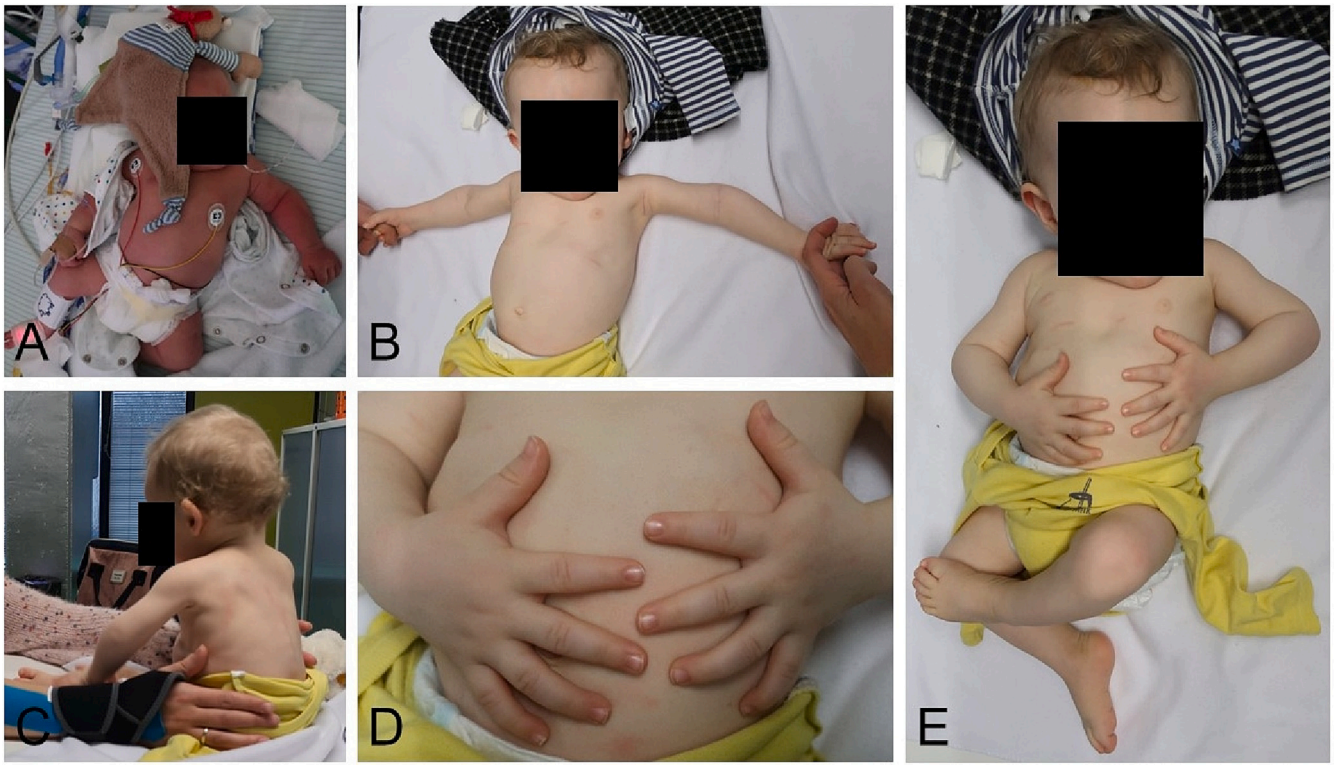

Fig. 2. Photographs of the patient on the first day of life (A) and at ten months of age (B–E). At birth, our patient presented with shortened proximal extremities and a bell-shaped thorax (A). In the further course, his growth was delayed, and he showed a significantly reduced body size (B–E).

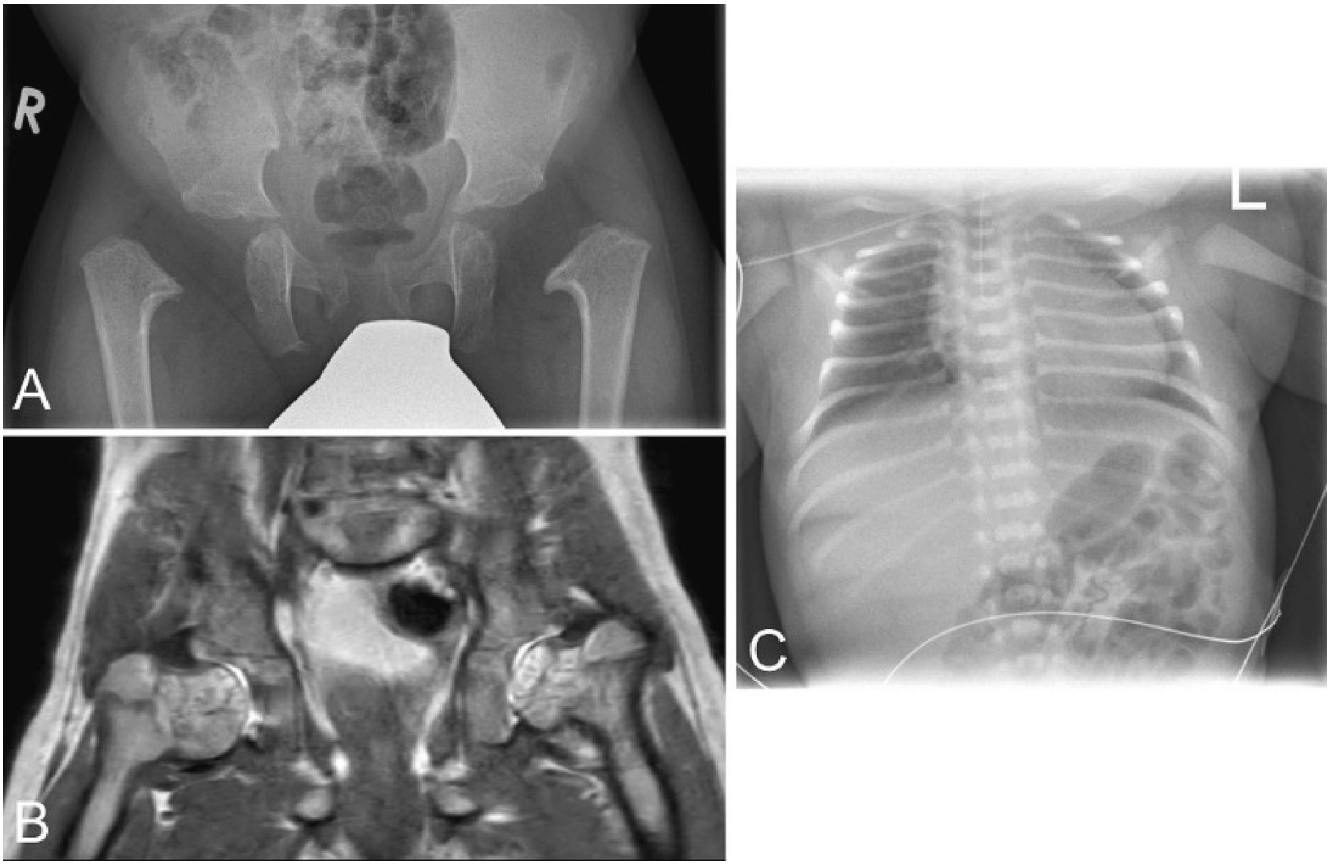

Fig. 3. Radiological examinations. (A, B) X-ray and MRI of the pelvis at 26 and 27 months, respectively. Conventional radiological examinations of the pelvis could not delimit epiphyseal nuclei and showed a regular horizontal position of the acetabulum without criteria of hip dysplasia. Coxa vara was confirmed in the subsequent MRI, where the whole femoral head and neck were cartilaginously created. (C) X-ray of the thorax of our patient on the first day of life. The thoracic bones did not show alterations.

3. Results and discussion

The diagnosis of SEMDDR was genetically confirmed when our patient was 16 months young. Whole exome sequencing revealed a heterozygous missense variant (NM_018359.3:c.905G>C, p.(Cys302Ser)) in the *UFSP2* gene. The variant was confirmed *de novo* in segregation analyses and was neither reported in databases (dbSNP, gnomAD, ClinVar) nor in the literature. According to ACMG criteria, the variant was likely pathogenic (PM1, PM2, PP3, PP5) concerning SEMDDR, an autosomal dominant hereditary disease (Di Rocco et al., 2018). Also, disease-causing variants were not identified in more than 500 genes related to more than 700 SDs (Unger et al., 2023).

The clinical presentation of our patient corresponds to the symptoms described in patients with SEMD. Patients usually become apparent with disproportionate short stature and epimetaphyseal dysplasia. Complications, such as premature osteoarthritis and atlantoaxial instability, may occur during the disease. SEMDDR is a subgroup of SEMD, first described by Di Rocco et al., caused by a heterozygous missense variant in the *UFSP2* gene (NM_018359.3:c.1277A>C, p.(Asp426Ala)) (Di Rocco et al., 2018). Here, a three-year-old Italian girl presented with short stature, waddling gait, mild genu varum, and leg pain. Radiological examinations revealed epiphyseal and metaphyseal dysplasia. Her mother and grandmother showed similar symptoms and had to undergo hip joint replacement at 27/28 years and 48/49 years, respectively. The second report of a missense variant in the *UFSP2* gene (NM_018359.3:c.1283A>G, p.(His428Arg)) in combination with similar symptoms is about an eight-year-old Chinese boy with progressive lesions in vertebrae, pelvis, and ankle as well as mild facial dysmorphism (Zhang et al., 2020). Initially, a heterozygous missense variant (NM_018359.3:c.868T>C, p.(Tyr290His)) affecting the *UFSP2* gene was identified in a large South African family of European descent with BHD (Watson et al., 2015). In contrast to SEMDDR, BHD is characterized by isolated premature degenerative osteoarthritis of the hip joints lacking additional skeletal anomalies. An overview of pathogenic variants in the *UFSP2* gene related to SD and the respective clinical features is given in Table 1.

All of the *UFSP2* variants related to SD are located in the C-terminal catalytic domain of UFSP2 (Fig. 1A, C). UFSP2 participates in UFM1 maturation and therefore plays a significant role in the UFM1 pathway, which is involved in various diseases because of its diverse functions in the cell cycle, *e.g.*, DNA repair, autophagy, and ER stress response (Witting and Mulder, 2021). Pathogenic variants in two of three components of the catalytic triad (Asp426 and His428) have already been associated with patients with SEMDDR (Di Rocco et al., 2018; Zhang et al., 2020). We here describe a patient with SEMDDR and a variant in the third part of the catalytic triad (Cys302). This supports the importance of a completely intact active site of UFSP2 for physiological bone development.

The Cys302 residue is highly conserved across species (Fig. 1B), and previous studies revealed a complete loss of UFSP2 function when the conserved cysteine residue was replaced by serine (Kang et al., 2007). Although the codon of Cys302 is located in exon 8 of the *UFSP2* gene, thus within the same exon as the BHD-related Tyr290, the phenotype of Cys302-related SD is similar to SEMDDR caused by pathogenic variants in Asp426 and His428 located in exon 11. The three-dimensional structure of UFSP2 (Fig. 1A), where the residues are in close relation to each other in the active site, and the identification of the catalytic triad consisting of Cys302, Asp426, and His428 corresponds to the clinical presentation of a more severe phenotype when components of

Table 1
Genetic and clinical data of our patient compared to the patients of Zhang et al. (2020), Di Rocco et al. (2018), Cilliers and Beighton (1990), and Watson et al. (2015).

	Our patient	Patient of Zhang et al.	Patients of Di Rocco et al.	Patients of Cilliers and Beighton and Watson et al.
Identified mutations	NM_018359.3:c.905G>C p.(Cys302Ser) Exon 8 (hg38)	NM_018359.3:c.1283A>G p.(His428Arg) Exon 11 (hg38)	NM_018359.3:c.1277A>C p.(Asp426Ala) Exon 11 (hg38)	NM_018359.3:c.868T>C p.(Tyr290His) Exon 8 (hg38)
Zygosity	Heterozygous	Heterozygous	Heterozygous	Heterozygous
Diagnosis	Spondyloepimetaphyseal dysplasia, Type di Rocco (SEMDDR) (OMIM# 617974)	Spondyloepimetaphyseal dysplasia, Type di Rocco (OMIM# 617974)	Spondyloepimetaphyseal dysplasia, Type di Rocco (OMIM# 617974)	Beukes hip dysplasia (BHD) (OMIM# 142669)
Inheritance	Autosomal dominant (*de novo*)	Autosomal dominant (*de novo*)	Autosomal dominant (inherited)	Autosomal dominant (inherited)
Further genetic tests	Exclusion of Kagami-Ogata syndrome, *SHOX* deletion, normal Array-CGH	Gene screening for dwarfism: heterozygous variant c.1198G>A (p. Ala400Thr) of the *GALNS* gene (NM_000512) not the primary cause of the patient's symptoms	/	Chromosomes normal in ten affected individuals
Sex	Male	Male	Three females (a girl, her mother, and grandmother)	24 females, 23 males
Time of birth	Born at term	Born at term	Girl born at 33rd gestational week	/
Height at birth (cm)	49	50	45 (65th percentile)	/
Height (Z-score)	−1.06	−0.22	/	/
Weight at birth (g)	3585	3300	2020 (45th percentile)	/
Weight (Z-Score)	0.38	−0.05	/	/
Head circumference at birth	37.5	/	/	/
Head circumference (Z-score)	2.39	/	/	/
Age at last examination	23 months	Eight years	Three years	/
Height (cm)	74	103	87.8	/
Height (Z-score)	−3.89	−5.06	−1.94	/
Clinical findings	Polyhydramnios, bell-shaped thorax, disproportionate rhizomelic short stature, genu varum, lumbar hyperlordosis, limited elbow extension, muscular hypotonia, gait instability	Short stature, waddling gait, genu varum, aggravation of growth disorder and joint pain with time, progressive lesions in vertebrae, pelvis, hip, femur, ankle	Girl: onset of leg pain in the second year of life, waddling gait, short stature, mild genu varum 38-year-old mother: 135 cm (SDS -4.5), congenital luxation of the hip at birth, waddling gait and painful joints with restricted mobility in childhood, genu varum since the age of 5 years, hip replacements at the age of 27 and 28 years 67-year-old grandmother: 142 cm (SDS -3.7), waddling gait, painful joints with restricted mobility since childhood, genu varum since the age of 10 years, hip joint replacement at the age of 48 and 49 years	Hip discomfort (before age two years in 24 persons, one at the age of 35 years), progressive deterioration, gait disturbance, secondary degenerative arthropathy in early adulthood, average stature, minimal involvement of other joints and the vertebral bodies (except for one young adult with severe kyphoscoliosis that necessitated spinal fusion), prosthetic joint replacement in some adults
Facial dysmorphism	/	Nasal bridge collapse, dysplasia of nostrils	/	/
Radiological findings	X-ray: bilateral epiphyseal nuclei of the femoral head conventional radiographically not delimitable, marked dysplasia of the metaphyses with malposition and misconfiguration of the metaphyseal areas of proximal bilateral femurs; no alterations of the thoracic bones MRI: deformed cartilaginous epiphyses of the proximal femurs, dysplastically deformed femoral metaphyses on both sides, no luxation, coxa vara	Delayed carpal bone age (progressively worsening), X-ray: backward protruding thoracic vertebrae, multiple fish mouth-like and bullet-like changes in thoracic and lumbar vertebrae, widening of the anterior segments of multiple ribs, deformed pelvis, shallow and irregular acetabulum bilateral, epiphysis of bilateral femoral head not delimitable, upper end of femur shifted irregularly outward and upward, ischemic necrosis of epiphysis of bilateral femoral head and dislocation of bilateral hip joint were suspected, slight swelling and deformity of shoulder and elbow joints, talus and calcaneus irregularly shaped	Girl: absence of ossification nucleus of the proximal femoral epiphysis, irregular profile of femur neck and acetabular roof, metaphyseal dysplasia of distal femur and proximal tibia, mild vertebral abnormalities, absence of epi- and metaphyseal anomalies in upper limbs, delayed carpal bone age Mother: absence of femoral capital epiphysis, metaphyseal involvement of distal femur and proximal tibia and vertebral bodies slightly flattened, coxa vara, osteoarthropathy in particular of wrist and shoulder, progressive spine involvement	Early childhood: broadening of the femoral necks, late appearance of the secondary ossification center of the femoral head, irregular appearance of the proximal epiphyseal line of the femur Mid childhood: flat femoral heads (coxa plana) with broadening of the femoral necks, adaptation of the acetabulum to the malformed femoral head, supero-lateral displacement of the femoral head, irregular appearance of the greater trochanteric epiphyses Adulthood: coxa plana,

(*continued on next page*)

Table 1 (*continued*)

	Our patient	Patient of Zhang et al.	Patients of Di Rocco et al.	Patients of Cilliers and Beighton and Watson et al.
				broadening of the neck, adaptation of the acetabulum to the malformed femoral head, shallow acetabulum with superior migration, superior migration and supero-lateral displacement of the femoral head, overgrowth of the greater trochanter in a supero-medial direction, early signs of secondary osteoarthrosis Older adult patients: more advanced secondary osteoarthrosis with pronounced periarticular cyst formation and prominent periarticular sclerosis, extreme narrowing of the joint space, severe destruction of the femoral head
Motor development	Delayed	Normal	Normal	/
Cognitive and speech development	Normal	Normal	Normal	/

the catalytic triad are affected. Looking in more detail at the catalytic reaction, the catalytic cysteine is responsible for a nucleophilic attack on the carbonyl carbon of the peptide bond, the histidine facilitates a proton transfer, and the transition state is stabilized by the aspartate (Ha et al., 2011). In contrast, Tyr290 is part of the oxyanion hole, another vital component of the active site formed by the backbone amide of tyrosine and catalytic cysteine. Oxyanion holes are present in papain-like proteases, such as cysteine proteases, serine proteases, and lipases, and stabilize the oxyanion transition state during the catalytic reaction. However, the exact molecular mechanism of SD caused by impaired UFSP2 function has not been deciphered yet. From genotype-phenotype correlations, we can assume that pathogenic variants affecting the catalytic triad lead to a more severe phenotype (SEMDDR) than variants in Tyr290, which participates in forming the oxyanion hole. There are similarities between BHD and SEMDDR regarding radiographic alterations of the femoral head and neck and the proximal femoral epiphysis, resulting in premature degenerative osteoarthritis of the hip joints. In contrast, patients with SEMDDR additionally show metaphyseal dysplasia, more frequent vertebral involvement and lesions affecting additional parts of the skeletal system, such as ribs, pelvis, and ankle. An essential difference between those two *UFSP2*-related entities is disproportionate short stature, which is only present in SEMDDR.

Identifying the genotype of patients with SE(M)D helps establish a definite diagnosis, as there is a phenotypic overlap between the different entities. For example, autosomal dominant *COL2A1*-related spondyloepiphyseal dysplasia congenita (SEDC, OMIM# 183900) (Terhal et al., 2015) and SEMD-S (Tiller et al., 1995) are characterized by neonatal severe disproportionate short stature and short extremities. Hypoplastic epiphyses of the long bones and poor ossification of the pubic bones and the vertebrae are radiographic features of both SEDC and SEMD-S. At the same time, only patients with SEMD-S develop metaphyseal dysplasia in the first year of life. Coxa vara, which occurred in our patient and one individual with SEMDDR reported by Di Rocco et al. (Di Rocco et al., 2018), is also known in patients with SEMD-S. Considering the radiographic characteristics (coxa vara, epiphyseal and metaphyseal dysplasia) and the clinical presentation (*e.g.*, disproportionate short stature), the phenotype of SEMD-S and SEMDDR overlaps to a certain extent. However, patients with SEMD-S (and SEDC) show characteristic facial features (hypertelorism, flat profile, Pierre Robin sequence), myopia, and hearing loss, all of which are absent in SEMDDR. Currently, it is not clear whether *UFSP2*-related SEMD entails the risk of atlantoaxial instability found in patients with SEMD-S (Amirfeyz et al., 2006). Nonetheless, this possibly life-threatening complication should be considered in patients with SEMDDR, taking into account the phenotypic overlap of those two entities.

Long-term support of patients with BHD and SEMDDR requires particular attention to premature osteoarthritis, as many adults had to undergo early prosthetic joint replacement. In addition, joint pain must be evaluated and treated to avoid a significant reduction in quality of life. Facial dysmorphism was not observed in patients with SEMDDR except for the eight-year-old Chinese boy, who presented with nasal bridge collapse and dysplasia of the nostrils (Zhang et al., 2020). Whether the polyhydramnios and the bell-shaped thorax observed in our patient at birth, as well as the delayed motor development and mild muscular hypotonia, are related to the identified likely pathogenic *UFSP2* variant remains unclear. Those additional clinical features might be considered specific for pathogenic *UFSP2* variants affecting the catalytic Cys302; however, this supposition has to be proven by further evaluation of patients with similar genetic alterations.

In summary, this is the first report of a patient diagnosed with autosomal dominant SEMD caused by a likely pathogenic variant affecting the catalytic Cys302 of *UFSP2*. Given the different clinical and radiological features of the distinct pathogenic *UFSP2* variants, the description of our patient will help improve the characterization, diagnosis, and clinic accompaniment for patients with *UFSP2*-related SD. Clinical follow-up studies are required to maintain targeted support for patients with SEMDDR, also in adulthood.

Accession numbers

National Center for Biotechnology Information. ClinVar; [VCV001098423.2], https://www.ncbi.nlm.nih.gov/clinvar/variation/VCV001098423.2 (accessed Nov. 17, 2022).

CRediT authorship contribution statement

Larissa Mattern: Writing – review & editing, Writing – original draft, Visualization, Investigation. **Matthias Begemann:** Writing –

review & editing, Visualization, Formal analysis. **Heide Delbrück:** Writing – review & editing, Visualization. **Petra Holschbach:** Writing – review & editing. **Silvia Schröder:** Writing – review & editing. **Sabine M. Schacht:** Writing – review & editing. **Ingo Kurth:** Writing – review & editing, Resources. **Miriam Elbracht:** Writing – review & editing, Supervision, Conceptualization.

Declaration of competing interest

None.

Data availability

The data that has been used is confidential.

Acknowledgement

Written informed consent was obtained from the parents for publication of this case report.

References

Amirfeyz, R., Taylor, A., Smithson, S.F., Gargan, M.F., 2006. Orthopaedic manifestations and management of spondyloepimetaphyseal dysplasia strudwick type. J. Pediatr. Orthop. B 15, 41–44. https://doi.org/10.1097/01202412-200601000-00009.

Brown, N.P., Leroy, C., Sander, C., 1998. MView: a web-compatible database search or multiple alignment viewer. Bioinformatics 14, 380–381. https://doi.org/10.1093/bioinformatics/14.4.380.

Cilliers, H.J., Beighton, P., 1990. Beukes familial hip dysplasia: an autosomal dominant entity. Am. J. Med. Genet. 36, 386–390. https://doi.org/10.1002/ajmg.1320360403.

Di Rocco, M., Rusmini, M., Caroli, F., Madeo, A., Bertamino, M., Marre-Brunenghi, G., Ceccherini, I., 2018. Novel spondyloepimetaphyseal dysplasia due to UFSP2 gene mutation. Clin. Genet. 93, 671–674. https://doi.org/10.1111/cge.13134.

Guo, Y., Ding, X., Shen, Y., Lyon, G.J., Wang, K., 2015. SeqMule: automated pipeline for analysis of human exome/genome sequencing data. Sci. Rep. 5, 14283. https://doi.org/10.1038/srep14283.

Ha, B.H., Jeon, Y.J., Shin, S.C., Tatsumi, K., Komatsu, M., Tanaka, K., Watson, C.M., Wallis, G., Chung, C.H., Kim, E.E., 2011. Structure of ubiquitin-fold modifier 1-specific protease UfSP2. J. Biol. Chem. 286, 10248–10257. https://doi.org/10.1074/jbc.M110.172171.

Jumper, J., Evans, R., Pritzel, A., Green, T., Figurnov, M., Ronneberger, O., Tunyasuvunakool, K., Bates, R., Žídek, A., Potapenko, A., Bridgland, A., Meyer, C., Kohl, S.A.A., Ballard, A.J., Cowie, A., Romera-Paredes, B., Nikolov, S., Jain, R., Adler, J., Back, T., Petersen, S., Reiman, D., Clancy, E., Zielinski, M., Steinegger, M., Pacholska, M., Berghammer, T., Bodenstein, S., Silver, D., Vinyals, O., Senior, A.W., Kavukcuoglu, K., Kohli, P., Hassabis, D., 2021. Highly accurate protein structure prediction with AlphaFold. Nature 596, 583–589. https://doi.org/10.1038/s41586-021-03819-2.

Kang, S.H., Kim, G.R., Seong, M., Baek, S.H., Seol, J.H., Bang, O.S., Ovaa, H., Tatsumi, K., Komatsu, M., Tanaka, K., Chung, C.H., 2007. Two novel ubiquitin-fold modifier 1 (Ufm1)-specific proteases, UfSP1 and UfSP2. J. Biol. Chem. 282, 5256–5262. https://doi.org/10.1074/jbc.M610590200.

Komatsu, M., Chiba, T., Tatsumi, K., Iemura, S., Tanida, I., Okazaki, N., Ueno, T., Kominami, E., Natsume, T., Tanaka, K., 2004. A novel protein-conjugating system for Ufm1, a ubiquitin-fold modifier. EMBO J. 23, 1977–1986. https://doi.org/10.1038/sj.emboj.7600205.

Li, M.-X., Gui, H.-S., Kwan, J.S.H., Bao, S.-Y., Sham, P.C., 2012. A comprehensive framework for prioritizing variants in exome sequencing studies of mendelian diseases. Nucleic Acids Res. 40, e53 https://doi.org/10.1093/nar/gkr1257.

Ni, M., Afroze, B., Xing, C., Pan, C., Shao, Y., Cai, L., Cantarel, B.L., Pei, J., Grishin, N.V., Hewson, S., Knight, D., Mahida, S., Michel, D., Tarnopolsky, M., Poduri, A., Rotenberg, A., Sondheimer, N., DeBerardinis, R.J., 2021. A pathogenic UFSP2 variant in an autosomal recessive form of pediatric neurodevelopmental anomalies and epilepsy. Genet Med. 23, 900–908. https://doi.org/10.1038/s41436-020-01071-z.

Pettersen, E.F., Goddard, T.D., Huang, C.C., Couch, G.S., Greenblatt, D.M., Meng, E.C., Ferrin, T.E., 2004. UCSF Chimera–a visualization system for exploratory research and analysis. J. Comput. Chem. 25, 1605–1612. https://doi.org/10.1002/jcc.20084.

Ren, J., Wen, L., Gao, X., Jin, C., Xue, Y., Yao, X., 2009. DOG 1.0: illustrator of protein domain structures. Cell Res. 19, 271–273. https://doi.org/10.1038/cr.2009.6.

Richards, S., Aziz, N., Bale, S., Bick, D., Das, S., Gastier-Foster, J., Grody, W.W., Hegde, M., Lyon, E., Spector, E., Voelkerding, K., Rehm, H.L., 2015. ACMG laboratory quality assurance committee, standards and guidelines for the interpretation of sequence variants: a joint consensus recommendation of the American College of Medical Genetics and Genomics and the Association for Molecular Pathology. Genet Med. 17, 405–424. https://doi.org/10.1038/gim.2015.30.

Terhal, P.A., Nievelstein, R.J.A.J., Verver, E.J.J., Topsakal, V., van Dommelen, P., Hoornaert, K., Le Merrer, M., Zankl, A., Simon, M.E.H., Smithson, S.F., Marcelis, C., Kerr, B., Clayton-Smith, J., Kinning, E., Mansour, S., Elmslie, F., Goodwin, L., van der Hout, A.H., Veenstra-Knol, H.E., Herkert, J.C., Lund, A.M., Hennekam, R.C.M., Mégarbané, A., Lees, M.M., Wilson, L.C., Male, A., Hurst, J., Alanay, Y., Annerén, G., Betz, R.C., Bongers, E.M.H.F., Cormier-Daire, V., Dieux, A., David, A., Elting, M.W., van den Ende, J., Green, A., van Hagen, J.M., Hertel, N.T., Holder-Espinasse, M., den Hollander, N., Homfray, T., Hove, H.D., Price, S., Raas-Rothschild, A., Rohrbach, M., Schroeter, B., Suri, M., Thompson, E.M., Tobias, E.S., Toutain, A., Vreeburg, M., Wakeling, E., Knoers, N.V., Coucke, P., Mortier, G.R., 2015. A study of the clinical and radiological features in a cohort of 93 patients with a COL2A1 mutation causing spondyloepiphyseal dysplasia congenita or a related phenotype. Am. J. Med. Genet. A 167, 461–475. https://doi.org/10.1002/ajmg.a.36922.

Tiller, G.E., Polumbo, P.A., Weis, M.A., Bogaert, R., Lachman, R.S., Cohn, D.H., Rimoin, D.L., Eyre, D.R., 1995. Dominant mutations in the type II collagen gene, COL2A1, produce spondyloepimetaphyseal dysplasia, strudwick type. Nat. Genet. 11, 87–89. https://doi.org/10.1038/ng0995-87.

Unger, S., Ferreira, C.R., Mortier, G.R., Ali, H., Bertola, D.R., Calder, A., Cohn, D.H., Cormier-Daire, V., Girisha, K.M., Hall, C., Krakow, D., Makitie, O., Mundlos, S., Nishimura, G., Robertson, S.P., Savarirayan, R., Sillence, D., Simon, M., Sutton, V.R., Warman, M.L., Superti-Furga, A., 2023. Nosology of genetic skeletal disorders: 2023 revision. Am. J. Med. Genet. A. https://doi.org/10.1002/ajmg.a.63132.

Watson, C.M., Crinnion, L.A., Gleghorn, L., Newman, W.G., Ramesar, R., Beighton, P., Wallis, G.A., 2015. Identification of a mutation in the ubiquitin-fold modifier 1-specific peptidase 2 gene, UFSP2, in an extended south african family with beukes hip dysplasia. S. Afr. Med. J. 105, 558–563. https://doi.org/10.7196/SAMJnew.7917.

Witting, K.F., Mulder, M.P.C., 2021. Highly specialized ubiquitin-like modifications: shedding light into the UFM1 enigma. Biomolecules 11, 255. https://doi.org/10.3390/biom11020255.

Zhang, G., Tang, S., Wang, H., Pan, H., Zhang, W., Huang, Y., Kong, J., Wang, Y., Gu, J., Wang, Y., 2020. UFSP2-related spondyloepimetaphyseal dysplasia: a confirmatory report. Eur. J. Med. Genet. 63, 104021 https://doi.org/10.1016/j.ejmg.2020.104021.